

Research Paper

Comparative Mitogenomic Analyses of Praying Mantises (Dictyoptera, Mantodea): Origin and Evolution of Unusual Intergenic Gaps

Hong-Li Zhang^{1*}, Fei Ye^{2, 3, 4*}✉

1. School of Life Sciences, Datong University, Datong 037009, China;
2. College of Ecology and Evolution, School of Life Sciences, Sun Yat-sen University, Guangzhou 510275, China;
3. State Key Laboratory of Biocontrol, Sun Yat-sen University, Guangzhou 510275, China;
4. College of Life Sciences, Shaanxi Normal University, Xi'an 710062, China.

* These authors contributed equally to this work.

✉ Corresponding author: feiyeemail@gmail.com

© Ivyspring International Publisher. This is an open access article distributed under the terms of the Creative Commons Attribution (CC BY-NC) license (<https://creativecommons.org/licenses/by-nc/4.0/>). See <http://ivyspring.com/terms> for full terms and conditions.

Received: 2016.07.30; Accepted: 2016.11.20; Published: 2017.02.25

Abstract

Praying mantises are a diverse group of predatory insects. Although some Mantodea mitogenomes have been reported, a comprehensive comparative and evolutionary genomic study is lacking for this group. In the present study, four new mitogenomes were sequenced, annotated, and compared to the previously published mitogenomes of other Mantodea species. Most Mantodea mitogenomes share a typical set of mitochondrial genes and a putative control region (CR). Additionally, and most intriguingly, another large non-coding region (LNC) was detected between *trnM* and *ND2* in all six Paramantini mitogenomes examined. The main section in this common region of Paramantini may have initially originated from the corresponding control region for each species, whereas sequence differences between the LNCs and CRs and phylogenetic analyses indicate that LNC and CR are largely independently evolving. Namely, the LNC (the duplicated CR) may have subsequently degenerated during evolution. Furthermore, evidence suggests that special intergenic gaps have been introduced in some species through gene rearrangement and duplication. These gaps are actually the original abutting sequences of migrated or duplicated genes. Some gaps (G5 and G6) are homologous to the 5' and 3' surrounding regions of the duplicated gene in the original gene order, and another specific gap (G7) has tandem repeats. We analysed the phylogenetic relationships of fifteen Mantodea species using 37 concatenated mitochondrial genes and detected several synapomorphies unique to species in some clades.

Key words: Mantodea, Mitochondrial genome, Control region (CR), Large non-coding region (LNC), Intergenic gap, Phylogeny.

Introduction

The Mantodea (praying mantis) contain more than 2,300 species with diverse morphologies and ecologies. These species occupy a diverse array of habitats, including tropical rainforests, temperate and arid forests and deserts, and employ different hunting strategies [1, 2]. Praying mantises have important applied value in pharmacy, agronomy, biological research and visualization, and most studies have primarily focused on their biological properties, such

as taxonomy and distribution, captive breeding, and application as a foodstuff [3-5].

The mitochondrial genome (mitogenome), as a powerful molecular marker [6, 7], has recently been used in preliminary study of the phylogenetic relationships among species from Mantodea [8]. In addition to the application in phylogeny, the mitogenome can provide a number of genome-level and evolutionary features, e.g. different

mitochondrial gene contents and orders in Mantodea [8]. A comprehensive and systematic study of mitogenome data, however, has not been explored for this group. When changes occur in gene content or gene order, a number of various intergenic gaps are introduced, which may hide the details of the change scenario. Thus, whether these special intergenic gaps are correlated with gene changes should be analysed and verified. Certain other specific regions in the Mantodea mitogenome also need further analysis, e.g., one large non-coding region (LNC) between *trnM* and *ND2* has been reported in *Tamolanica tamolana* (Brancsik, 1897) and *Hierodula formosana* Giglio-Tos, 1912 [9, 10]. Two control regions (CRs) in the mitogenome have been reported in a few groups, including sea cucumbers, birds, snakes, fish, thrips, ticks, and tortoises [11-17]. The duplicated CR is extremely similar to the original CR in most cases, suggesting that both CRs are evolving in concert. However, both CRs in some species of birds and tortoises appear to be independently evolving [17, 18]. It is unknown if the specific LNC of some mantodean mitogenomes is another degenerated control region, and the evolutionary patterns of the LNC and CR are unclear.

In the present study, we described four new mitogenomes from Paramantini and conducted a comparative analysis on all available mitogenomes from fifteen species representing four families of Mantodea. These studies included comprehensive analyses on the features of protein-coding genes (PCGs), structural features in transfer RNAs (tRNAs) and ribosomal RNAs (rRNAs), structural elements in the control regions, and the phylogenetic relationships of these species based on 37 concatenated mitochondrial genes. Moreover, we examined the potential origin and evolutionary features of LNCs in Paramantini mitogenomes and the special intergenic gaps introduced by gene changes.

Material and Methods

Specimen sampling and DNA extraction

Adult specimens of *Hierodula patellifera* (Serville, 1839), *Rhombodera brachynota* (Wang & Dong, 1993), *Rhombodera valida* Burmeister, 1838 and *Rhombodera* sp. were collected from Shaanxi and Yunnan Province, China, and the voucher specimens for the four species were deposited in Shaanxi Normal University (Table S1). All collections were preserved in 95% ethanol and stored at -20°C for the preservation of nucleic acids. For each species, total genomic DNA was extracted from the leg muscle tissue using a TIANamp Micro DNA Kit (Tiangen Biotech, Beijing, China).

PCR amplification and sequencing of mitogenome

Four entire mitogenomes were amplified with overlapping PCR fragments using a series of universal primer sets [19] and species-specific primers designed according to the newly acquired sequence fragments (Table S2). The PCR reactions were essentially performed as previously described [8]. All purified PCR products were directly sequenced from both strands at the Beijing Genomics Institute (BGI) using the ABI 3730XL Genetic Analyser (PE Applied Biosystems) with a primer-walking strategy.

Mitogenome annotation and bioinformatics analyses

Raw sequences were assembled using Staden package 1.7.0 [20]. Most of the tRNAs from four species were identified using tRNAscan-SE 1.21 [21], which was also used to predict the secondary structure of tRNAs. The remaining tRNAs, 13 PCGs and two rRNAs were identified after alignment with the genes of other Mantodea species [8]. The secondary structures of the small ribosomal subunit (*rrnS*) and the large ribosomal subunit (*rrnL*) for *R. brachynota* were predicted according to the models for *Drosophila virilis* Sturtevant, 1916 and *Drosophila melanogaster* Meigen, 1830, respectively [22, 23]. The nucleotide composition and codon usage were analysed using Mega 5.0 [24]. DnaSP 5.1.0 [25] was used to calculate the rates of non-synonymous substitutions (K_a), the rates of synonymous substitutions (K_s), the codon bias index (CBI), the effective number of codons (ENC), the G+C content of all codons (G+C), and the G+C content of the third codon sites ((G+C)₃). Tandem repeat (TDR) sequences in CRs and LNCs were identified using Tandem Repeat Finder 4.09 [26], and we predicted the potential secondary structures of the repeat unit using the Mfold 3.1.2 [27].

Phylogenetic analyses

All 37 mitochondrial genes were selected to analyse the phylogenetic relationship among fifteen Mantodea species (Table 1). Two termite species, *Macrotermes natalensis* (Haviland, 1898) (GenBank accession numbers: NC_025522) and *Coptotermes lacteus* (Froggatt, 1898) (GenBank accession numbers: NC_018125), were selected as outgroups. Each PCG was aligned based on amino acid sequence alignment using MEGA 5.0. Both rRNA and tRNA genes were aligned using Clustal X 1.83 [28]. The alignments of 37 genes were subsequently concatenated as a combined matrix (mtDNA) using Bioedit 7.0 [29]. The partitioning scheme (each codon site of PCGs; tRNA and rRNA genes) was employed for the dataset

mtDNA. Furthermore, we reconstructed the phylogenetic relationship using two other datasets: the CCR, the relatively conserved region of the CR in each family; and the LNC_CR, LNCs from six Paramantini species and CRs from all Mantodea species. These two datasets (CCR and LNC_CR) were respectively aligned using Clustal X 1.83. The GTR+I+ Γ was selected as the optimal model for all four partitions (mtDNA) and the other datasets (CCR and LNC_CR) according to the Akaike information criterion in MODELTEST v.3.7 [30] and MrModeltest 2.3 [31]. Bayesian inference (BI) analyses were performed using MrBayes 3.1.2 [32] with four MCMC chains running for five million generations. Each set was sampled every 1000 generations. The first 25% of steps were discarded as burn-in. Maximum Likelihood (ML) analyses were implemented in RAxML 7.0.3 [33], and the nodal support values among branches were assessed through bootstrap analysis with 1000 replicates.

Table 1. List of Mantodea species included in the present study.

Family	Species	Accession number	Reference
Hymenopodidae	<i>Anaxarcha zhengi</i> Ren & Wang, 1994	KU201320	[8]
	<i>Creobroter gemmatus</i> (Stoll, 1813)	KU201319	[8]
Mantidae	<i>Tenodera sinensis</i> Saussure, 1871	KU201318	[8]
	<i>Tamolana tamolana</i> (Brancsik, 1897)	DQ241797	[9]
	<i>Hierodula formosana</i> Giglio-Tos, 1912	KR703238	[10]
	<i>Hierodula patellifera</i> (Serville, 1839)	KX611803	This study
	<i>Rhombodera brachynota</i> (Wang & Dong, 1993)	KX611802	This study
	<i>Rhombodera valida</i> Burmeister, 1838	KX611804	This study
	<i>Rhombodera</i> sp.	KX619654	This study
Liturgusidae	<i>Mantis religiosa</i> Linnaeus, 1758	KU201317	[8]
	<i>Statilia</i> sp.	KU201316	[8]
	<i>Humbertiella nada</i> Zhang, 1986	KU201315	[8]
	<i>Theopompa</i> sp.-HN	KU201313	[8]
Tarachodidae	<i>Theopompa</i> sp.-YN	KU201314	[8]
	<i>Leptomantella albella</i> (Burmeister, 1838)	KJ463364	[34]

Results

Mitogenome features of newly sequenced Mantodea species

The complete mitogenomes of *R. brachynota*, *H. patellifera*, *R. valida* and *Rhombodera* sp. were 16,616, 16,999, 16,308 and 15,910 bp in size, respectively (GenBank accession numbers: KX611802, KX611803, KX611804 and KX619654, respectively) (Table 2). The four mitogenomes contained a typical set of 37 mitochondrial genes (13 PCGs, 22 tRNAs, and two rRNAs) and retained identical gene order with most sequenced Mantodea mitogenomes [8]. In addition to the classic control region, the other large non-coding regions (LNCs) were detected between *trnM* and

ND2. The four Mantodea mitogenomes were consistently biased towards A and T (~ 75.0%). Among the four major molecules (PCGs, rRNAs, tRNAs, and CR), the CR displayed the highest A+T content in three species, with *R. valida* as the exception, in which the CR intriguingly displayed the lowest A+T content (Table S3). All features of the nucleotide composition detected in these four mitogenomes were similar to those observed in other Mantodea species [8]. In the four newly sequenced mitogenomes, all PCGs were initiated with a canonical ATN codon (N represents any one of four nucleotides, A, T, C, G), with the exception of *COI* using TTG and CTG as initiation codons. The conventional TAA codon was used as a termination codon in most of the PCGs of these Mantodea mitogenomes, and the incomplete termination codons T and TA were also detected in two PCGs, *COII* and *ND5*, respectively (Table 2).

Comparative mitogenomic analyses of the fifteen Mantodea species

Protein-coding genes

Comparative analyses revealed the consistent characteristics and evolutionary patterns of 13 PCGs for praying mantis mitogenomes. All PCGs were AT biased in all fifteen Mantodea species. The PCGs encoded by the majority strand (PCGs-J) and the minority strand (PCGs-N) displayed moderate C-skews and marked G-skews (>0.200), respectively, and both strands displayed T-skews (Table S3). The low ω value (Ka/Ks<0.3) for each PCG revealed that all PCGs might have evolved under strong purifying selection. In addition, the highest ω value was observed for *ATP8*, implying that *ATP8* evolved at a fast rate (Fig. S1).

The most frequently used codon was NNU (45.0%) in all PCGs and PCGs-N, while NNA (44.0%) was the most abundant in PCGs-J (Table S4). The codons ending with A/U were favoured for both the four-fold and two-fold degenerate codons (Fig. 1). Four AT-rich codons, UUU (Phe), UUA (Leu), AUU (Ile), and AUA (Met) were the most prevalent codons in all fifteen Mantodea mitogenomes, with values ranging from 26.6% in *Humbertiella nada* Zhang, 1986 to 37.2% in *Anaxarcha zhengi* Ren & Wang, 1994 (Table S5). The usage proportion of the four AT-rich codons was positively correlated with the A+T content of PCGs ($R^2 = 0.973$) in the fifteen Mantodea species (Fig. S2). Furthermore, the codon usage bias was associated with the G+C content of PCGs. ENC was positively correlated with G+C ($R^2 = 0.979$) and (G+C)₃ ($R^2 = 0.994$), and conversely, CBI was negatively correlated with both G+C and (G+C)₃ and also with ENC ($R^2 = 0.988$) (Fig. S3).

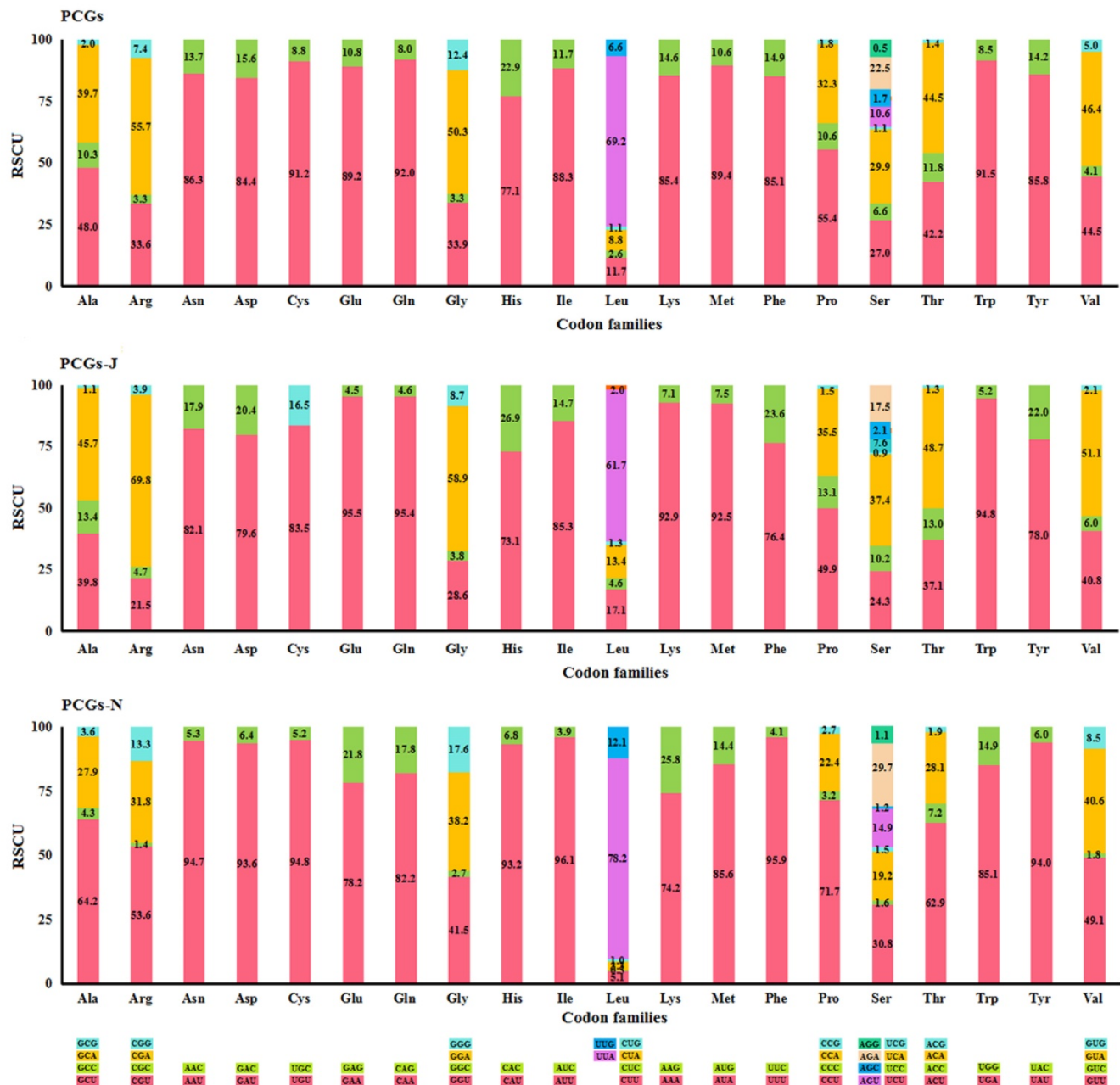


Figure 1. Percentage of synonymous codon usage of each amino acid in the fifteen Mantodea mitogenomes. PCGs-J: PCGs encoded by the majority strand. PCGs-N: PCGs encoded by the minority strand.

Table 2. Annotation of the four praying mantis mitogenomes.

Gene (region)	Coding Strand	<i>Hierodula patellifera</i>	<i>Rhombodera brachynota</i>	<i>Rhombodera valida</i>	<i>Rhombodera</i> sp.				
		Position	Position	Position	Position				
		Start/stop codon	Start/stop codon	Start/stop codon	Start/stop codon				
<i>trnI</i>	J	1-66	1-66	1-66	1-66				
<i>trnQ</i>	N	76-144	72-140	71-139	71-139				
<i>trnM</i>	J	144-212	140-209	139-206	139-208				
<i>ND2</i>	J	1754-2782	ATG/TAA	1381-2409	ATG/TAA	763-1791	ATT/TAA	669-1697	ATG/TAA
<i>trnW</i>	J	2781-2851		2408-2478		1791-1861		1696-1765	
<i>trnC</i>	N	2844-2908		2471-2534		1854-1917		1758-1821	
<i>trnY</i>	N	2909-2977		2535-2605		1918-1986		1822-1890	
<i>COI</i>	J	2982-4517	TTG/TAA	2610-4145	CTG/TAA	1993-3528	TTG/TAA	1896-3431	CTG/TAA
<i>trnL^{UUR}</i>	J	4524-4591		4152-4219		3536-3603		3438-3504	
<i>COII</i>	J	4596-5280	ATG/T	4224-4908	ATG/T	3607-4291	ATG/T	3510-4194	ATG/T
<i>trnK</i>	J	5281-5352		4909-4980		4292-4363		4195-4266	

Gene (region)	Coding Strand	<i>Hierodula patellifera</i>		<i>Rhombodera brachynota</i>		<i>Rhombodera valida</i>		<i>Rhombodera</i> sp.	
		Position	Start/stop codon	Position	Start/stop codon	Position	Start/stop codon	Position	Start/stop codon
<i>trnD</i>	J	5354-5419		4983-5048		4367-4432		4269-4334	
<i>ATP8</i>	J	5420-5578	ATT/TAA	5049-5207	ATT/TAA	4433-4591	ATC/TAA	4335-4493	ATC/TAA
<i>ATP6</i>	J	5572-6252	ATG/TAA	5201-5881	ATG/TAA	4585-5265	ATG/TAA	4487-5167	ATG/TAA
<i>COIII</i>	J	6255-7043	ATG/TAA	5884-6672	ATG/TAA	5268-6056	ATG/TAA	5170-5958	ATG/TAA
<i>trnG</i>	J	7046-7110		6675-6739		6059-6124		5961-6025	
<i>ND3</i>	J	7111-7464	ATT/TAA	6740-7093	ATT/TAA	6125-6478	ATT/TAA	6026-6379	ATT/TAA
<i>trnA</i>	J	7472-7536		7100-7164		6489-6554		6390-6454	
<i>trnR</i>	J	7541-7607		7169-7236		6559-6624		6459-6526	
<i>trnN</i>	J	7607-7671		7236-7300		6624-6689		6526-6591	
<i>trnS^{AGN}</i>	J	7672-7738		7301-7367		6690-6756		6592-6658	
<i>trnE</i>	J	7740-7806		7369-7435		6758-6823		6660-6725	
<i>trnF</i>	N	7807-7871		7440-7504		6824-6890		6727-6791	
<i>ND5</i>	N	7871-9591	ATA/TA	7504-9224	ATA/TA	6890-8613	ATG/TA	6791-8514	ATG/TA
<i>trnH</i>	N	9595-9658		9228-9291		8614-8677		8515-8578	
<i>ND4</i>	N	9662-10999	ATG/TAA	9295-10632	ATG/TAA	8682-10019	ATG/TAA	8582-9919	ATG/TAA
<i>ND4L</i>	N	10993-11274	ATG/TAA	10626-10907	ATG/TAA	10013-10294	ATG/TAA	9913-10194	ATG/TAA
<i>trnT</i>	J	11281-11344		10912-10975		10299-10362		10199-10262	
<i>trnP</i>	N	11345-11407		10976-11038		10363-10425		10263-10326	
<i>ND6</i>	J	11410-11913	ATT/TAA	11041-11544	ATT/TAA	10428-10931	ATT/TAA	10329-10832	ATT/TAA
<i>CytB</i>	J	11913-13049	ATG/TAA	11544-12680	ATG/TAA	10931-12067	ATG/TAA	10832-11968	ATG/TAA
<i>trnS^{UCN}</i>	J	13049-13118		12681-12750		12067-12136		11969-12038	
<i>ND1</i>	N	13143-14078	ATG/TAA	12769-13704	ATG/TAA	12164-13099	ATG/TAA	12058-12993	ATG/TAG
<i>trnL^{CUN}</i>	N	14080-14147		13706-13773		13101-13168		12995-13062	
<i>rrnL</i>	N	14148-15462		13774-15087		13169-14485		13063-14377	
<i>trnV</i>	N	15463-15532		15088-15157		14486-14555		14378-14447	
<i>rrnS</i>	N	15533-16326		15158-15947		14556-15349		14448-15238	
CR	—	16327-16999		15948-16616		15350-16308		15239-15910	

J: the majority strand; N: the minority strand; CR: control region.

Transfer RNAs

We calculated the percentage of identical nucleotides (%INUC) for each tRNA family of the fifteen Mantodea mitogenomes. Two tRNAs (*trnY* and *trnL^{CUN}*), located on the minority strand, displayed low levels of conservation (%INUC < 50.0%). Five tRNAs (*trnI*, *trnA*, *trnN*, *trnF* and *trnS^{UCN}*) showed high levels of conservation (%INUC > 75.0%), and the majority strand encoded four of these tRNAs (Table S6). Thus, the conservation pattern of tRNA genes was distinct in the two coding strands. Additional analyses of the conservation of stems and loops in the secondary structure of tRNAs revealed that nucleotides in the amino acid acceptor stem (AA stem), the dihydrouridine stem (DHU stem) and the anticodon stem (AC stem) are relatively conserved (>70.0%). Among the four loops, only the anticodon loop exhibited high sequence similarity (87.0%) (Fig. 2 & Table S6).

Ribosomal RNAs

The *rrnS* of *R. brachynota* comprised three structural domains (I-III) (Fig. 3A). The conserved sites were marked and analysed within the fifteen Mantodea species. In the eight helices of domain I

(H9-H511), H47 was the most unstable. Domain II, containing five helices (H567-H885), was the most highly variable domain, particularly for helices H567, H577 and H673. In domain III, most helices were relatively conserved, except for H1068-H1113 and H1303 (Table S7). The *rrnL* of *R. brachynota* harboured five canonical structural domains (I-II, IV-VI) (Fig. 3B). The conserved sites in *rrnL* of the fifteen Mantodea species were also analysed. Five helices were observed in Domain I, which were difficult to align. Nonetheless, H563 was correspondingly stable (75.0%). Domain II comprised 14 helices (H579-H1196), and the conservation level was high in H671, H777, and H1087 (>75.0%) (Table S7). All helices in Domains IV and V were relatively conserved, except for helices H1648, H1764, H2077, H2259, H2395, and H2520 (<40.0%) (Table S7). Furthermore, eight couplets were observed in H1792, but not as frequently as the five couplets observed in most insects [35]. Although nucleotides in the variable helices were highly divergent at the family and even subfamily levels, most of these molecules are compensatory base changes and shared some similar secondary structures among the species. In Domain VI, all three helices were changeable.

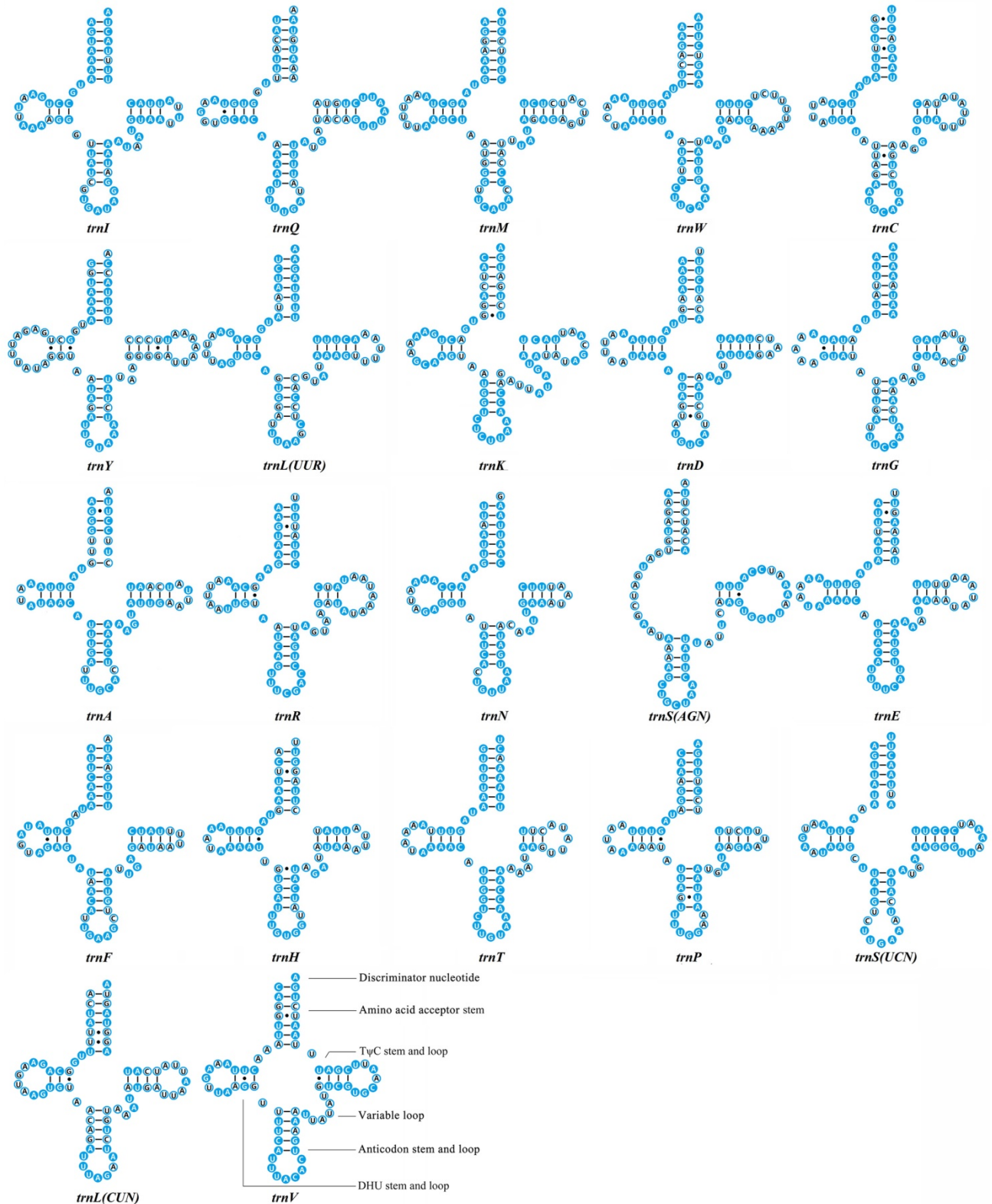
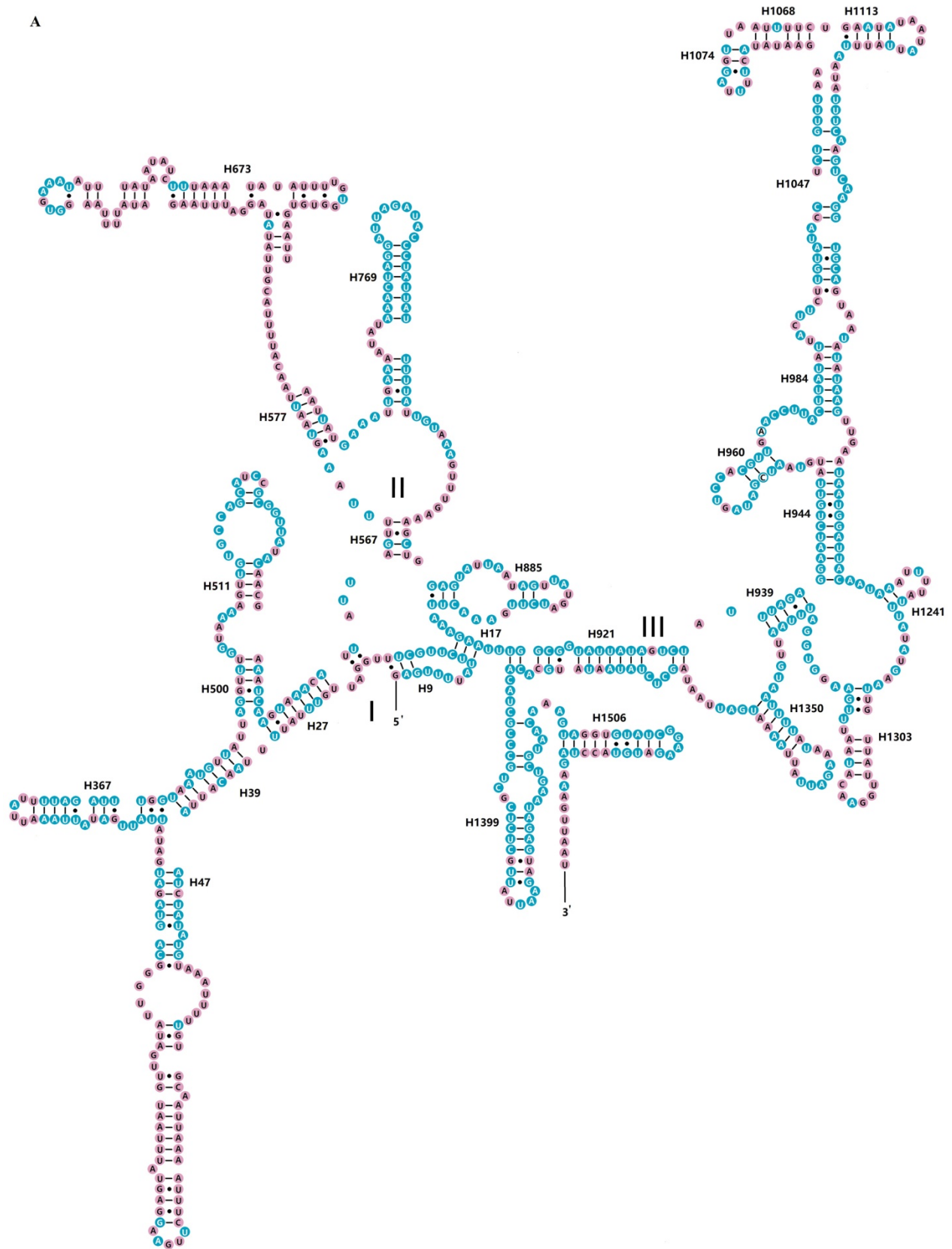


Figure 2. Inferred secondary structures of 22 transfer RNAs (tRNAs) identified in *Rhombodera brachynota*. Conserved sites within the fifteen Mantodea species are indicated as white nucleotides within blue spheres. Variable sites are indicated as black nucleotides within blue circles. Bars: Watson-Crick base pairings. Dots: GU base pairings.



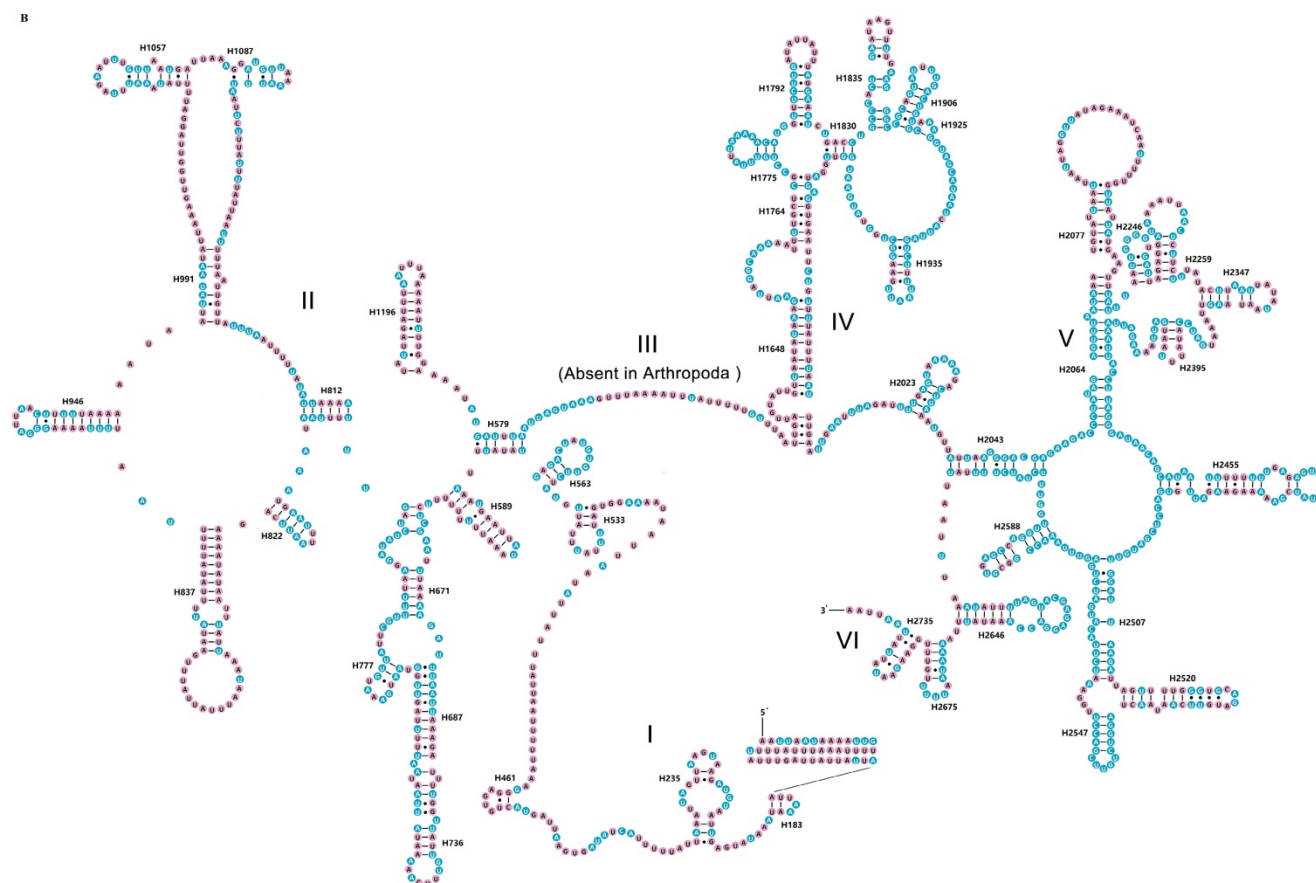


Figure 3. Inferred secondary structures of two ribosomal RNAs in *Rhombodera brachynota*. (A) *rrnS*. (B) *rrnL*. Conserved sites within fifteen Mantodea species are indicated as white nucleotides within blue spheres. Variable sites are indicated as black nucleotides within pink spheres. Bars: Watson-Crick base pairings. Dots: GU base pairings.

Control region

The CR is located in the conserved position at the downstream of *rrnS* for all sequenced Mantodea mitogenomes. The length is relatively variable in this region, ranging from 639 bp in *Mantis religiosa* Linnaeus, 1758 to 1,775 bp in *Theopompa* sp.-HN, with most of the size variation being attributed to the presence of TDRs (Table S8). The alignment of the CRs from these Mantodea mitogenomes (removing redundant TDRs) did not reveal the typical conserved element information of the insect control region. Nevertheless, excluding *T. tamolana*, two conserved block sequences (CBS1: ATACGWATAATRTAM(T)A TAAATCTT and CBS2: TTATTATA) and one Poly-T (>7 bp) were observed in the other fourteen Mantodea mitogenomes (the Poly-T was separated by one C in *Statilia* sp.) (Fig. 4A, 4B & Table S8). In addition, the flanking regions of this Poly-T were relatively conserved. The consensus motif “AGXTT(Y/-)CA” was observed at the 5’ end, except for *Statilia* sp., and one succeeding “(A/-)AATGRA” motif was present at the 3’ end of this Poly-T (Fig. 4A). Moreover, the CRs of species from the same family were aligned (without

the single representative species of Tarachodidae), and one relatively conserved region of CR (CCR) was observed in three families. The size and sequence similarity of this region were different in the three families: 205 bp (78.5%) in Hymenopodidae, 257 bp (82.5%) in Liturgusidae, and 237 bp (58.2%) in Mantidae, except for *T. tamolana*. Further alignment of the CRs of species from the same tribe showed that the CCR had increased in size (~ 300 bp), and the identity of this region was also increased (>75.0%) (Table 3). With the brief partitioning scheme of CR without redundant TDRs: three equal sections (5’ end, middle, 3’ end), CCRs in the Hymenopodidae and Mantidae were located at the latter half of the middle and the first half of the 3’ end in CRs, while CCRs in Liturgusidae were focused on the middle section of CRs (Fig. 4 & Table 3). Despite the alignment of the CCRs from three families, there remained only two CBSs. The corresponding conserved regions for the single representative species of Tarachodidae, *Leptomantella albella* (Burmeister, 1838), were also detected after alignment with CRs from three Liturgusidae species.

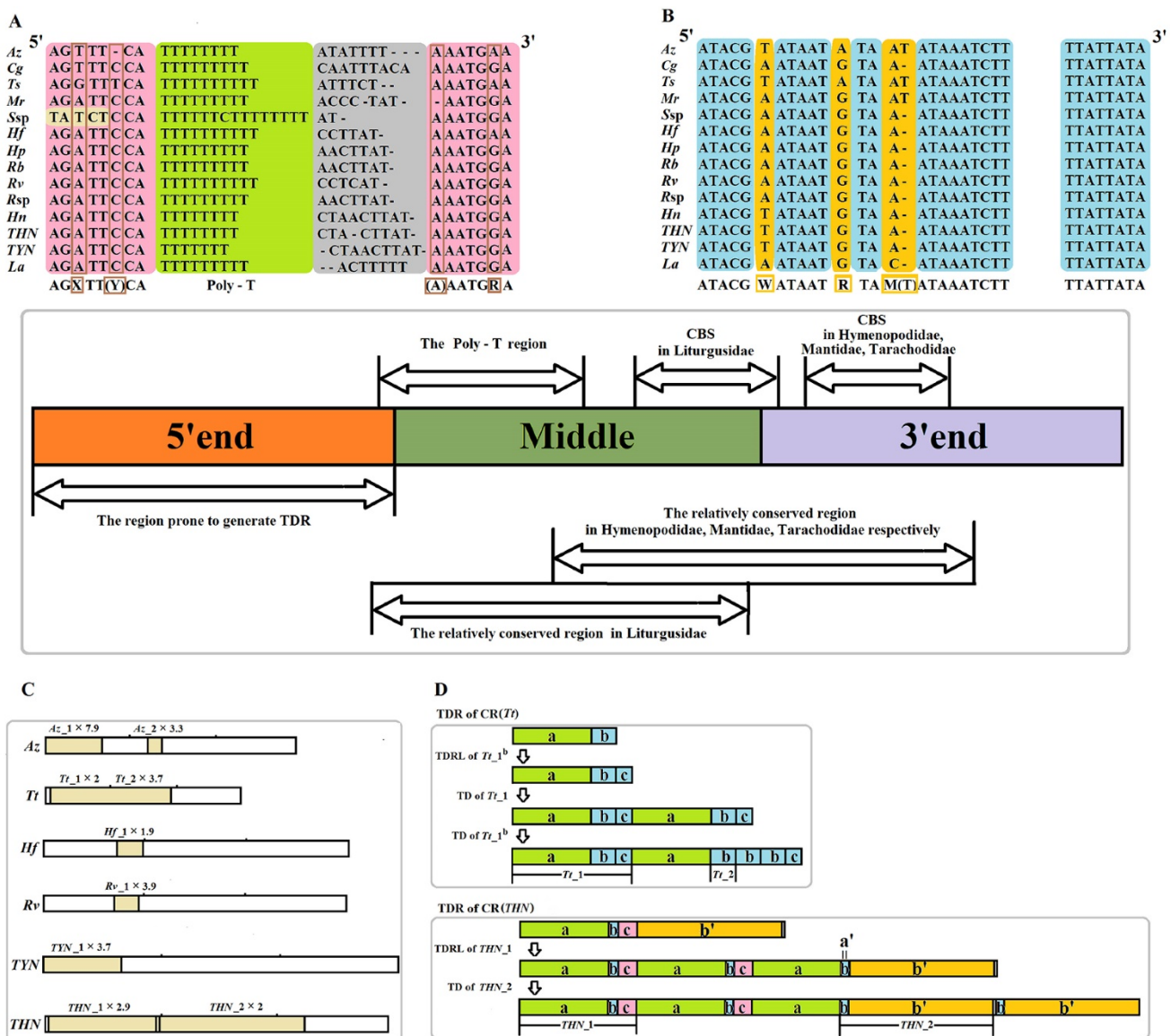


Figure 4. Organization of the control region (CR) in fifteen Mantodea mitogenomes. Redundant TDRs were removed in the partitioning of CR. (A) Poly-T region in the majority strand. Poly-T structure is indicated with a light green background; the flanking regions of poly-T in the majority strand are indicated with a pink background; the variable site in the flanking region is indicated with a brown frame. (B) Two conserved block sequences (CBS1 and CBS2) in the majority strand. Conserved sites in the CBSs are indicated with a blue background, and the variable site in the CBSs is indicated with an orange background. (C) Tandem repeats (TDRs) of CRs in six Mantodea species. (D) The possible repeat mechanism of TDRs in CR (Tt) and CR (THN). TDRL: tandem duplication-random loss. TD: tandem duplication. Az: *Anaxarcha zhengi*. Cg: *Creobroter gemmatus*. Ts: *Tenodera sinensis*. Tt: *Tamolanica tamolana*. Hf: *Hierodula formosana*. Hp: *Hierodula patellifera*. Rb: *Rhombodera brachynota*. Rv: *Rhombodera valida*. Rsp: *Rhombodera* sp. Mr: *Mantis religiosa*. Ssp: *Statilia* sp. Hn: *Humbertiella nada*. THN: *Theopompa* sp.-HN. TYN: *Theopompa* sp.-YN. La: *Leptomantella albella*.

In the CRs of fifteen Mantodea species, TDRs were only observed in six species, displaying variable sized repeat units, spanning from 40 bp in Az_2 to 396 bp in THN_2. Although TDRs primarily occurred at the 5' end, TDRs were also detected in the middle section of CRs in three species (Fig. 4C & Table 4). Most TDRs repeated less than three times, but the repetitive unit of Az_1 repeated seven times. The occurrence of TDRs was not correlated with the nucleotide composition of the repetitive unit, including the A+T content, AT-skew and GC-skew. Repeat units from the same TDRs in CRs displayed extremely high sequence homology (>95.0%) (Table 4), which may indicate that the rate of copy turnover

is higher relative to the rate of nucleotide substitution because the homogenization or divergence between repeats primarily depends on the rate of copy addition and deletion (copy turnover) relative to the nucleotide mutation rate [36]. Furthermore, all repetitive unit sequences could be folded into the secondary structure with two or more stem-loops (Fig. S4). These repeat units could form stable secondary structures during strand slippage, which may facilitate the generation of tandem repeats [37], and these structures may promote replication slippage through the inhibition of the polymerase or stabilization of the slipped strand [38].

Table 3. The position and conservation rate of the relatively conserved region of control region (CCR) in each family and tribe.

Family/Tribe	Speices	Position* of conserved region	Alignment size (bp)	Conserved site (nt)	Conservation rate (%)
Hymenopodidae	<i>Anaxarcha zhengi</i>	330-534	205	161	78.5
	<i>Creobroter gemmatus</i>	391-592			
Mantidae	<i>Tenodera sinensis</i>	365-594	237	138	58.2
	<i>Tamolonica tamolana</i>	-			
	<i>Hierodula formosana</i>	453-680			
	<i>Hierodula patellifera</i>	340-566			
	<i>Rhombodera brachynota</i>	345-570			
	<i>Rhombodera valida</i>	436-665			
	<i>Rhombodera</i> sp.	336-563			
	<i>Mantis religiosa</i>	303-531			
	<i>Statilia</i> sp.	311-541			
Liturgusidae	<i>Humbertiella nada</i>	268-563	257	212	82.5
	<i>Theopompa</i> sp.-HN	307-602			
	<i>Theopompa</i> sp.-YN	300-592			
Tarachodidae	<i>Leptomantella albella</i>	255-556	298	234	78.5
Paramantini (Mantidae)	<i>Hierodula formosana</i>	389-681			
	<i>Hierodula patellifera</i>	275-567			
	<i>Rhombodera brachynota</i>	279-571			
	<i>Rhombodera valida</i>	371-666			
Mantini (Mantidae)	<i>Rhombodera</i> sp.	272-564	342	263	76.9
	<i>Mantis religiosa</i>	205-535			
	<i>Statilia</i> sp.	206-545			

Position*: position in CR without redundant TDRs.

Table 4. Statistics of TDRs in the CRs and LNCs of Mantodea mitogenomes.

Region (Species abbreviation)	Size	TDRs	Positions	Consensus size (bp)	Copy number	Percent Matches (%)	AT%	AT-skew	GC-skew	Number of Hairpin	Average ΔG
CR(Az)	1761	Az_1	1-1181	149	7.9	100	75.8	0.080	0.072	4	18.3
		Az_2	1290-1419	40	3.3	100	95.0	-0.053	0	2	1.8
CR(Tt)	954	Tt_1	15-622	305	2	98.0	74.4	0.075	0.080	9	26.6
		Tt_2	521-750	63	3.7	98.0	63.5	-0.150	0.025	2	5.7
CR(TYN)	1436	TYN_1	1-732	200	3.7	100	66.5	-0.023	0.221	6	7.9
CR(THN)	1775	THN_1	9-785	271	2.9	99.0	64.9	-0.114	-0.017	9	22.6
		THN_2	776-1561	396	2	100	76.8	-0.105	0.073	8	45.8
CR(Hf)	840	Hf_1	192-317	65	1.9	100	56.9	0.189	-0.055	2	7.8
CR(Rv)	959	Rv_1	180-435	65	3.9	100	55.4	0.278	0.085	2	8.8
LNC(Hf)	625	LNC(Hf)_1	6-463	199	2.3	99.0	71.4	-0.056	0.021	6	19.2
LNC(Hp)	1541	LNC(Hp)_1	20-1371	180	7.5	100	68.9	-0.048	0.065	5	25.4
LNC(Rb)	1171	LNC(Rb)_1	17-1021	183	5.5	100	59.0	-0.019	0.028	7	20.8
LNC(Rv)	556	LNC(Rv)_1	20-262	65	3.7	100	69.4	-0.017	0.062	2	8.5

CR: control region; LNC: Large non-coding region between *trnM* and *ND2*; TDR: tandem repeat; ΔG : Gibbs free energy; Az: *Anaxarcha zhengi*; Tt: *Tamolonica tamolana*; THN: *Theopompa* sp.-HN; TYN: *Theopompa* sp.-YN; Hf: *Hierodula formosana*; Hp: *Hierodula patellifera*; Rb: *Rhombodera brachynota*; Rv: *Rhombodera valida*.

Furthermore, some TDRs shared an overlapping region, e.g., *Tt_2* overlaps 102 nucleotides with *Tt_1* (Fig. 4D & Table 4). Comparisons of these two repetitive units demonstrated that the *Tt_2* unit is a small part of the *Tt_1* unit (namely *Tt_1^b*), and the *Tt_1* unit could be divided into three parts (*Tt_1^a*, *Tt_1^b* and *Tt_1^c*), among which *Tt_1^c* is one section of *Tt_1^b*. The potential repeat process for this region may require three steps: 1) the original sequence comprising *Tt_1^a* and *Tt_1^b*. Firstly, *Tt_1^b* tandemly repeats during the slippage-strand mispairing of mtDNA replication, where only 41 bp (*Tt_1^c*) is reserved in the repeated sequence; 2) secondly, the *Tt_1* unit tandemly repeats one time; and 3) third, the *Tt_1^b* in the duplicated *Tt_1* unit is copied two more

times. Additionally, in *Theopompa* sp.-HN CR, *THN_2* overlaps ten nucleotides with *THN_1* (Fig. 4D & Table 4). In reality, the *THN_1* unit could be divided into three parts, *THN_1^a*, *THN_1^b* and *THN_1^c*; and the *THN_2* unit is actually 390 bp in size and could be divided into two parts, *THN_2^a* and *THN_2^b*. Among these subunits, *THN_2^a* is exactly the same as *THN_1^b*, therefore the tandem repeat in this region could be elucidated using the following process: 1) the *THN_1* unit is successively repeated twice, whereas *THN_1^c* is lost in the second repetitive process; 2) the second repeated *THN_1^b* and *THN_2^b* compose the repetitive unit of *THN_2*. *THN_2* is repeated once, but a gap (6 bp in size) exists between the two same repeat units.

Other non-coding regions

Apart from the typical control region, another large non-coding region (LNC) was also observed in all six Paramantini species. LNCs were located between *trnM* and *ND2*, with variable lengths ranging from 296 bp in *T. tamolana* to 1,541 bp in *H. patellifera*. TDRs can also be detected in LNCs from four species of Paramantini (Table 4).

Two unusual gaps were present between *trnM* and *trnI* (G1) and between *trnQ* and *ND2* (G2) in three Liturgusidae species (except for the undetermined junction of *trnM-trnI* in *Theopompa* sp.-HN) (Fig. 5A). Although the gene content has not changed in *Theopompa* sp.-YN, a 69-bp gap (G3) was detected between *trnA* and *trnR* in this species and appeared as the pseudogene *trnR* [8]. In addition, a 68-bp gap (G4) was detected between *trnR* and *trnN* in *Creobroter gemmatus* (Stoll, 1813), which could be the remnant of *trnR* [8]. Tandem duplications of *trnR* were primarily present in four species, *C. gemmatus*, *M. religiosa*, *Statilia* sp., and *Theopompa* sp.-HN. The gap sequence between duplicated *trnRs* was "ATTTAATTT" (G5) in

C. gemmatus. Within G5, "TTAATTT" is exactly identical to the fragment comprising the extremital three nucleotides (TTA) in *trnA* and the junction between *trnA* and *trnR* (ATTT). In addition, the main body of G5 also comprised the extremital two nucleotides of the junction between *trnR'* and *trnN* (AT) and the six nucleotides of the 5' end in *trnN* (TTAATT) (Fig. 5B). A 28-bp gap (G6) was observed between duplicated *trnRs* in *Theopompa* sp.-HN. This gap encompassed two parts (P1 and P2). P1 was the same as the junction sequence between *trnR* and *trnN*, and P2 was not only consistent with the beginning sequence of *trnN* but was also identical to the fragment comprising the extremital three nucleotides (TTG) in *trnA* and the junction sequence (ATTG) between *trnA* and *trnR* (Fig. 5B). A 19-bp gap (G7) was observed between duplicated *trnRs* in *M. religiosa*. A 17-bp gap (G8) was detected between duplicated *trnR/W₂* in *Statilia* sp., and the front six nucleotides (P1) in G8 were consistent with the gap sequence between *trnW₂* and *trnN* (Fig. 5B).

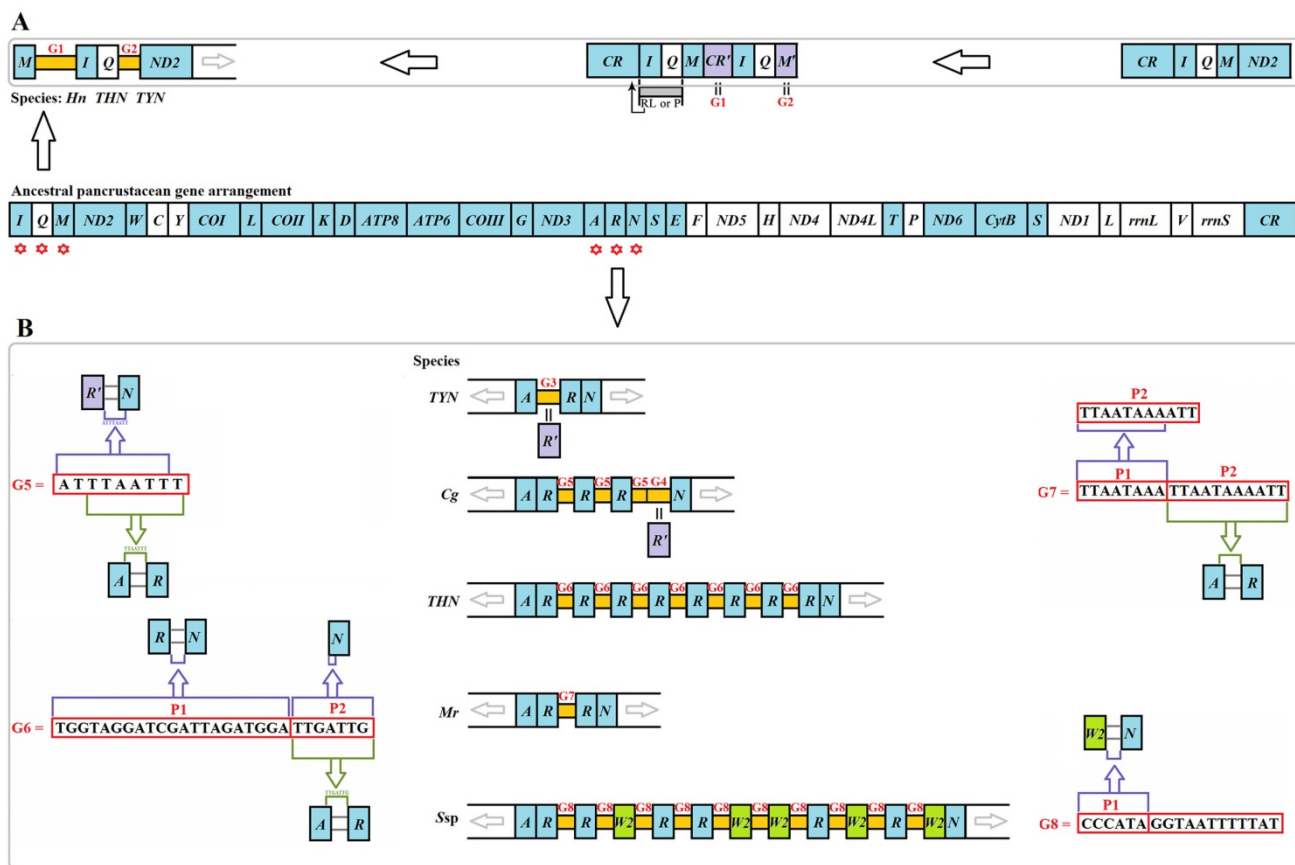


Figure 5. Intergenic gaps introduced by gene rearrangement and duplication. The gene and genome sizes are not to scale. The minority strand encodes all genes with white blocks, and the majority strand encodes all genes with blue blocks. (A) G1 and G2 introduced by gene rearrangement in three Liturgusidae mitogenomes. RL: random loss. P: pseudogenization (B) G3-G8 introduced by gene duplication in Mantodea mitogenomes. *Hn*: *Humbertiella nada*. *THN*: *Theopompa* sp.-HN. *TYN*: *Theopompa* sp.-YN. *Cg*: *Creobroter gemmatus*. *Mr*: *Mantis religiosa*. *Ssp*: *Statilia* sp.

Phylogenetic implications on Mantodea

Considering the phylogenetic results [8] and partitioning strategy [39-41] of previous studies, the phylogenetic analyses in the present study were performed on the partitioned dataset mtDNA of fifteen Mantodea species using two inference methods (Fig. 6A & Fig. S5). The phylogenies deduced using ML and BI showed almost identical topologies with high support values in most branches. Only *L. albella* representing Tarachodidae clustered with the three species of Liturgusidae in mtDNA-ML topology but with low support value (Fig. S5).

Discussion

The origin and evolution of degenerative control region

The LNCs from six Paramantini species showed low similarity, and only one short relatively conserved section was observed near *ND2*. The presence and variation in size and sequence of TDRs indicated that this unassigned region might be associated with the CR. When the redundant TDRs of LNC and CR were removed, the length of LNC was approximately half of the corresponding CR, and the identity of the aligned region was low (<60.0%), except for in *H. formosana* and *R. valida* (>70.0%). Nevertheless, one extremely conserved section (>90.0%) between LNC and CR was examined in *T. tamolana*, *H. formosana* and *R. valida*, respectively (Table 5). Successively, we divided the LNCs of these three species into several small sections, and each section was aligned with the remaining mitogenome sequence. The alignment results showed that most sections could be aligned to CR, while these

homologous regions were scattered through the whole CR. Furthermore, a tRNA-like structure was detected at the 3' end of LNCs in two *Rhombodera* species (Fig. S6). Although the anticodon of the tRNA-like structure could not be identified in *Rhombodera* sp., these two tRNA-like sequences exhibited high homology with *trnM*. The alignment of the same position (the extremital sequence of LNCs) of the other four Paramantini species and the remaining sequence of mitogenome for each species showed that *trnM* is also the most similar region for this small section, although the identity was low (~60.0%) (Table 5). Overall, with the exception of the small *trnM*-like section, the main body of LNC may be another degenerative control region, and LNCs may be a synapomorphy for Paramantini species.

The control region, the largest non-coding region in mitogenome, is involved in the regulation of replication and transcription of the mitogenome [42]. Therefore, the duplication and degeneration of this region may have important evolutionary significance. In most cases, there is only one control region in the mitogenome of insects, while two control regions have been detected in some species of thrips [15] and katydid [43]. Two mechanisms have been proposed for the occurrence of duplicate CRs in circular mitogenomes: (1) tandem duplication – the replication errors may bring two tandem-repeated sections in one mitogenome. If the errors occurred in the section including the CR, then each tandem-repeated section will contain a CR. (2) illegitimate recombination – a fragment including the CR was cleaved out from one mitogenome and subsequently introduced into another mitogenome.

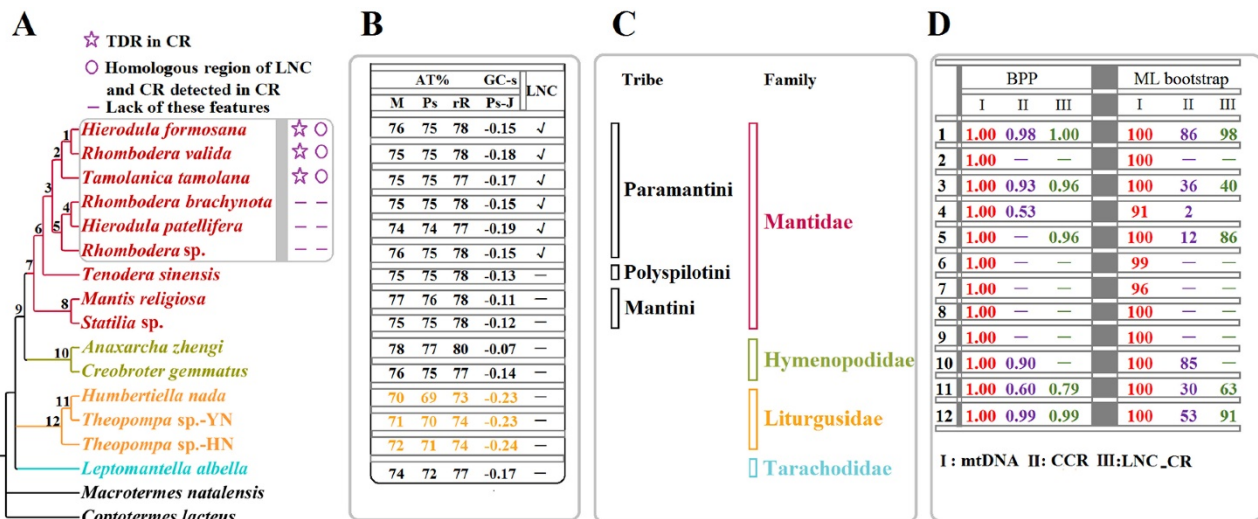


Figure 6. Phylogenetic relationship among the fifteen Mantodea species. (A) Phylogeny constructed using BI analyses based on mtDNA. TDR: tandem repeat. CR: control region. LNC: Large non-coding region between *trnM* and *ND2*. (B) The A + T content (AT%) and GC - skew (GC-s) of several portions in the mitogenomes of fifteen Mantodea species. M: mitogenome. Ps: Protein-coding genes. rR: rRNAs. Ps-J: Protein-coding genes encoded by the majority strand. ✓: LNCs. —: no LNCs. (C) The lineage of fifteen Mantodea species. (D) The branch support values in each node. BPP: Bayesian posterior probabilities.

Table 5. The comparison of LNC and CR from six Paramantini species.

Species	CR-TDR size (bp)	LNC-TDR size (bp)	Region (Species abbreviation)	Alignment of LNC(-TDR) and CR(-TDR)			Alignment of <i>trnM</i> -Like sequence in LNC and <i>trnM</i>		
				Alignment size (bp)	Conserved site (nt)	Conserved rate (%)	Total size (bp)	Conserved site (nt)	Conserved rate (%)
<i>Tamolonica tamolana</i>	498	296	SR(<i>Tt</i>)	299	169	56.5	78	47	60.3
			HCR(<i>Tt</i>)	56	55	98.2			
<i>Hierodula formosana</i>	779	366	SR(<i>Hf</i>)	384	271	70.6	72	48	66.7
			HCR(<i>Hf</i>)	191	185	96.9			
<i>Hierodula patellifera</i>	674	369	SR(<i>Hp</i>)	380	174	45.8	80	51	63.8
<i>Rhombodera brachynota</i>	669	349	SR(<i>Rb</i>)	384	174	45.3	71	41	57.7
<i>Rhombodera valida</i>	768	378	SR(<i>Rv</i>)	383	271	70.8	69	44	63.8
			HCR(<i>Rv</i>)	202	188	93.1			
<i>Rhombodera</i> sp.	672	460	SR(<i>Rsp</i>)	505	245	48.5	71	44	62.0

CR: control region; LNC: Large non-coding region between *trnM* and *ND2*; -TDR: redundant tandem repeats were removed; SR: similar region; HCR: highly conserved region; *Tt*: *Tamolonica tamolana*; *Hf*: *Hierodula formosana*; *Hp*: *Hierodula patellifera*; *Rb*: *Rhombodera brachynota*; *Rv*: *Rhombodera valida*; *Rsp*: *Rhombodera* sp.

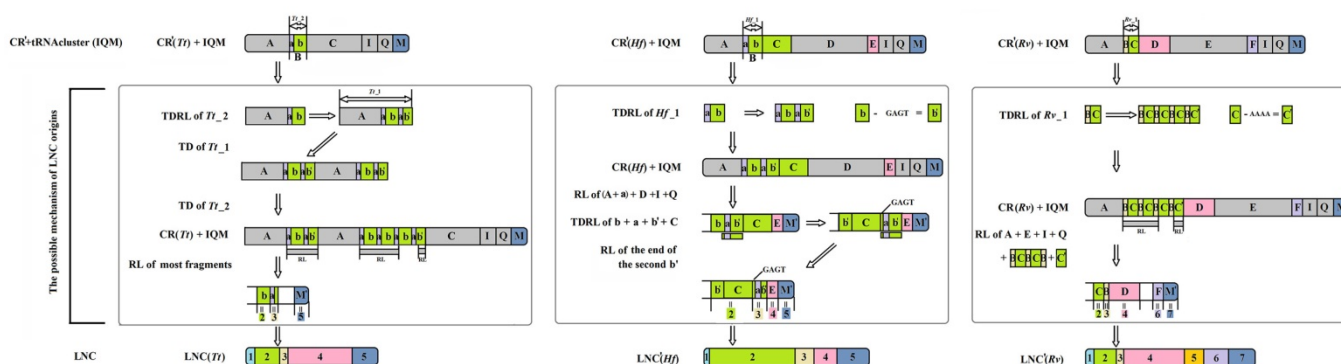


Figure 7. The possible mechanism for the origin of LNCs from *Tamolonica tamolana*, *Hierodula formosana* and *Rhombodera valida*. CR: control region. CR': CR without redundant tandem repeats. LNC: large non-coding region between *trnM* and *ND2*. LNC': LNC without redundant tandem repeats. TD: tandem duplication. RL: random loss. *Tt*: *Tamolonica tamolana*. *Hf*: *Hierodula formosana*. *Rv*: *Rhombodera valida*.

As a result, the recipient mitogenome will have two CRs. For Paramantini mitogenomes, the generated scenario of LNCs, however, might be complicated. It is plausible that the tandem duplication-random loss (TDRL) [44] accounts for the LNCs origin of *T. tamolana*, *H. formosana* and *R. valida* (Fig. 7). The initial repeat unit of TDR in CR or the current CR with TDR for these three species appears to have existed prior to the duplication of the whole CR to form the LNC. Based on this frame, we infer the potential generation of LNC and the present CR derived from assumed CR (without redundant TDR): the repeat unit of assumed CR was extended to form TDRs, and the whole CR (including TDRs) and tRNA cluster (*trnI-trnQ-trnM*) repeated together; subsequently, most spaced and tandem repeated fragments were randomly lost, and the several remaining parts in these fragment mutated and formed the heterogeneous region, viz. parts 1 and 4 in LNC(*Tt*), part 1 in LNC(*Hf*), and parts 1 and 5 in LNC(*Rv*) (Fig. 7). Generally, duplicate CRs evolve under two evolutionary pathways: concerted evolution and independent evolution [16]. In many cases, two CRs could easily be aligned, showing high

sequence similarity, and simultaneously, the conserved functional sequence elements were completely preserved in each copy, suggesting that the two CRs are evolving in concert [45]. Although most portions of LNCs from *T. tamolana*, *H. formosana* and *R. valida* could be detected in the CR, both LNCs and CRs are difficult to align as a whole and the aligned portions of the LNCs are scattered in CRs (Fig. 7).

Whether these LNCs evolved in concert with CRs is open to debate. Typically, section duplication in the mitogenome is followed by the deletion or degeneracy of one of the duplicated copies, and consequently the coexistence of duplicate regions was short lived on an evolutionary timescale [46], e.g., extremely divergent size and sequence between LNCs and CRs in *Rhombodera* sp., *H. patellifera* and *R. brachynota*, and both appeared to evolve independently (Table 5). Much higher resolution was achieved in the phylogenetic relationships based on the LNC_CR dataset (Fig. 8) with LNCs from all six Paramantini species and all 15 CRs clustering together, respectively. The separation between LNCs and CRs was well supported by predicted

phylogenetic relationships under this scenario (Fig. 8). If orthologous copies are more closely related than paralogous copies, then the two copies have evolved independently since prior to the speciation of the group [18], and indeed this was the conclusion deduced from phylogenetic results for all LNCs (Fig. 8). Therefore, these results suggest that all LNCs in these Paramantini species are independently evolving.

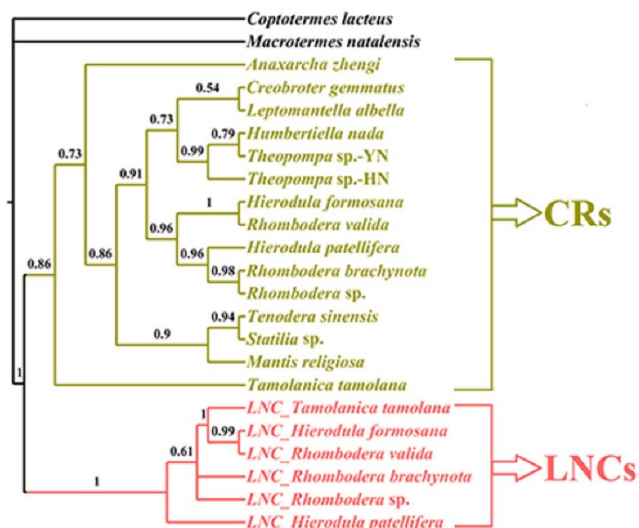


Figure 8. The phylogenetic relationship of LNCs and CRs using BI analyses. CR: control region. LNC: large non-coding region between *trnM* and *ND2*.

Intergenic gaps introduced through gene rearrangement and duplication

According to the gene rearrangement mechanism, TDRL model [44], G1 was most likely a small segment from the CR because when *trnI-trnQ-trnM* was tandemly duplicated, the small section abutting *trnI* may have duplicated along with the gene cluster (Fig. 5). G1 can also fold into many stem-loop structures (Fig. S7). However, the similarity was only approximately 45.0% in the aligned region between G1s and CRs from two Liturgusidae species, and the G1 sequences from two species also displayed low similarity (35.5%). Hence, G1 might have been derived from CR if mutations constantly accumulated in this gap along with the rearrangement process. G2 is a *trnM* pseudogene that has previously been reported [8]. G4 in *C. gemmatus* indicated that *trnR* duplicated three times, while the partial sequence of the AA stem was lost in the third copy, leading to the formation of the *trnR* pseudogene. The sequences of G5 and G6 demonstrated that the surrounding regions of the 5' and 3' of duplicated *trnR* harbour homologous fragments of the flanking sequences in the original order, which may be associated with the occurrence of the *trnR* duplication. The last 11 bp (P2)

in G7 are the same as the sequence of the distal three nucleotides (TTA) in the AA stem of *trnA* and the intergenic gap sequence between *trnA* and *trnR*. In addition, the first 9 bp (P1) is the incomplete copy of P2, suggesting that *trnR* has been duplicated twice, with a subsequent loss of only the first copy of *trnR* and three abutting nucleotides (ATT) (Fig. 5). Analysing the intergenic gap introduced by gene rearrangement and duplication revealed that the abutting sequence could also migrate or duplicate along with the gene changes. Based on these findings, we propose that the intergenic gap sequence between the changed genes may be used to explore the mechanism of gene rearrangement and duplication.

Phylogenetic analyses among fifteen species from Mantodea

In the phylogeny obtained in the present study, species representing Hymenopodidae and Mantidae grouped together as a sister group, while Liturgusidae and Tarachodidae formed independent lineages (Fig. 6A), similar to the phylogenetic relationships constructed using combined mitochondrial and nuclear sequence data [47,48]. Furthermore, the relationship among species from the same family or tribe is also consistent with the phylogeny based on these molecular data [47,48]. Within Liturgusidae, *Theopompa* sp.-YN clustered with *H. nada* and subsequently grouped with *Theopompa* sp.-HN. from the same genus, which has been previously verified [8]. For three species from Liturgusidae, *trnM* was translocated at the upstream of *trnI* and formed a novel gene order (*trnM-trnI-trnQ*). Additionally, compared with other Mantodea species, the whole mitogenome and three important gene types (PCGs, rRNAs and tRNAs) displayed lower A+T contents, and PCGs-J also possessed different levels of GC-skew (Fig. 6B), suggesting that these common features may be a synapomorphy of the Asian bark mantis. Within the Mantidae, *Tenodera sinensis* Saussure, 1871 representing Mantinae first clustered with six Paramantini species from Paramantinae as a sister group, and subsequently clustered with the remaining two species from Paramantinae (Fig. 6A). Paramantini was divided into two branches: *T. tamolana*, *H. formosana* and *R. valida* formed one clade (clade I), and the remaining species were grouped together as another clade (clade II), showing that the genera *Hierodula* and *Rhombodera* were not recovered as a monophyletic lineage respectively (Fig. 6A). Notably, the TDRs and the homologous region between LNC and CR were observed in the CRs of all three clade I species, while these features could not be preserved in the three species from clade II. This

raises a question: do apparently different features of CR and LNC from two clades represent the distinct evolutionary rates and patterns for CR and LNC in these two clades for Paramantini? This question deserves further assessment with a broader taxon sample. The phylogenetic relationship in Paramantini, with the exception of *T. tamolana*, was also supported by the phylogeny based on the relatively conserved region of CRs in each family (CCR dataset) (Fig. S8 & Fig. 6D).

Whether the CCR in each family possesses a phylogenetic signal for analysing the relationship of these Mantodea species is not clear. The phylogeny based on this region was reconstructed, and two species from Hymenopodidae clustered together. Three species from Liturgusidae also formed one small clade, and all their relationships were consistent with the phylogenetic results based on mtDNA. Although eight species from Mantidae were dispersed, six Paramantini species grouped together. In Paramantini, these species from *Hierodula* and *Rhombodera* promiscuously clustered together (Fig. S8), as found in the mtDNA phylogeny. These results may indicate that the relatively conserved region of CR in family may be used to analyse the phylogenetic relationship among species with close relationship.

Conclusion

In summary, four new mitogenomes of Paramantini were sequenced and annotated, and these mitogenomes shared the same gene content and gene order with most known Mantodea mitogenomes. We presented a comprehensive comparative analysis of fifteen Mantodea mitogenomes and obtained preliminary results for the mitogenome characteristics and evolutionary patterns. Most species displayed similar usage bias in nucleotides and codons. The relatively conserved and variable regions were unevenly distributed in the secondary structures of tRNAs and rRNAs. Three common elements, two CBSs and one poly-T, were found in CRs. LNCs in Paramantini may have initially originated from the CR, although the major intact homologous region is difficult to detect between CRs and LNCs generated through paralogous copies. Differing from two CRs evolving in concert in other species, the LNCs and CRs in this tribe independently evolved, which is supported by the phylogenetic relationship constructed using LNC_CR data. Some features in these intergenic gap sequences introduced by gene rearrangement and duplication may be helpful to characterize the mechanism of gene changes. Furthermore, phylogenetic analyses among fifteen Mantodea species suggest that the mitogenome

is a useful marker for resolving phylogenetic relationships among Mantodea species.

Abbreviations

Mitogenome: mitochondrial genome; LNC: large non-coding region between *trnM* and *ND2*; CR: control region; PCGs: protein-coding genes; CBS: conserved block sequence; tRNAs: transfer RNAs; rRNAs: ribosomal RNAs; Ka: the rates of non-synonymous substitutions; Ks: the rates of synonymous substitutions; CBI: the codon bias index; ENC: the effective number of codons; (G+C): the G+C content of all codons; (G+C)₃: the G+C content of the third codon sites; TDR: tandem repeat; CCR: the relatively conserved region of CR in each family; BI: Bayesian inference; ML: Maximum Likelihood; PCGs-J: PCGs encoded by the majority strand; PCGs-N: PCGs encoded by the minority strand; %INUC: the percentage of identical nucleotides; AA stem: the amino acid acceptor stem; DHU stem: the dihydrouridine stem; AC stem: the anticodon stem; *rrnS*: the small ribosomal subunit; *rrnL*: the large ribosomal subunit; G: intergenic gap; TDRL: tandem duplication-random loss.

Supplementary Material

Supplementary figures and tables.

<http://www.ijbs.com/v13p0367s1.pdf>

Acknowledgements

This study was supported by grants from the Doctoral Scientific Research Foundation of Datong University (No. 2013-B-08) and the National Natural Science Foundation of China (31372158). The authors would like to thank Dr. David Cone (Saint Mary's University) and Dr. Ping You (Shaanxi Normal University) for providing helpful comments on a previous draft of the manuscript.

Competing Interests

The authors have declared that no competing interest exists.

References

1. Ehrmann R. Mantodea: Gottesanbeterinnen der Welt. Münster, Germany: Natur und Tier Verlag; 2002.
2. Svenson GJ, Whiting MF. Phylogeny of Mantodea based on molecular data: evolution of a charismatic predator. *Systematic Entomology*. 2004; 29: 359-70.
3. Ramsay GW. Mantodea (Insecta), with a review of aspects of functional morphology and biology. *Fauna of New Zealand*. 1990; 19: 1-96.
4. Terra PS. Revisão sistemática dos generos de Louva-A-Deus da região Neotropical (Mantodea). *Revista Brasileira de Entomologia*. 1995; 39: 13-94.
5. Vanitha K, Bhat PS, Raviprasad TN, Srikumar KK. Biology and behaviour of *Ephestiasula pictipes* (Wood-Mason) (Hymenopodidae: Mantodea) under captive breeding. *International Journal of Pest Management*. 2016; 62: 308-18.
6. Boore JL. The use of genome-level characters for phylogenetic reconstruction. *Trends in Ecology & Evolution*. 2006; 21: 439-46.
7. Hirase S, Takeshima H, Nishida M, Iwasaki W. Parallel Mitogenome sequencing alleviates random rooting effect in phylogeography. *Genome Biology and Evolution*. 2016; 8: 1267-78.

8. Ye F, Lan XE, Zhu WB, You P. Mitochondrial genomes of praying mantises (Dictyoptera, Mantodea): rearrangement, duplication, and reassigment of tRNA genes. *Scientific Reports*. 2016; 6: 25634.
9. Cameron SL, Barker SC, Whiting MF. Mitochondrial genomics and the new insect order Mantophasmatodea. *Molecular Phylogenetics and Evolution*. 2006; 38: 274-9.
10. Tian X, Liu J, Cui Y, Dong P, Zhu Y. Mitochondrial genome of one kind of giant Asian mantis, *Hierodula formosana* (Mantodea: Mantidae). *Mitochondrial DNA* 2015; [Epub ahead of print].
11. Arndt A, Smith MJ. Mitochondrial gene rearrangement in the sea cucumber genus *Cucumaria*. *Molecular Biology and Evolution*. 1998; 15: 1009-16.
12. Eberhard JR, Wright TF, Bermingham E. Duplication and concerted evolution of the mitochondrial control region in the parrot genus *Amazona*. *Molecular Biology and Evolution*. 2001; 18: 1330-42.
13. Kumazawa Y, Ota H, Nishida M, Ozawa T. Gene rearrangements in snake mitochondrial genomes: highly concerted evolution of control-region-like sequences duplicated and inserted into a tRNA gene cluster. *Molecular Biology and Evolution*. 1996; 13: 1242-54.
14. Lee JS, Miya M, Lee YS, Kim CG, Park EH, Aoki Y, Nishida M. The complete DNA sequence of the mitochondrial genome of the self-fertilizing fish *Rivulus marmoratus* (Cyprinodontiformes, Rivulidae) and the first description of duplication of a control region in fish. *Gene*. 2001; 280: 1-7.
15. Shao R, Barker SC. The highly rearranged mitochondrial genome of the plague thrips, *Thrips imaginis* (Insecta: Thysanoptera): convergence of two novel gene boundaries and an extraordinary arrangement of rRNA genes. *Molecular Biology and Evolution*. 2003; 20: 362-70.
16. Shao R, Barker SC, Mitani H, Aoki Y, Fukunaga M. Evolution of duplicate control regions in the mitochondrial genomes of metazoa: a case study with Australasian Ixodes ticks. *Molecular Biology and Evolution*. 2005; 22: 620-9.
17. Zheng CF, Nie LW, Wang J, Zhou HX, Hou HZ, Wang H, Liu JJ. Recombination and evolution of duplicate control regions in the mitochondrial genome of the Asian big-headed Turtle, *Platysternon megacephalum*. *PLoS one*. 2013; 8: e82854.
18. Abbott CL, Double MC, Trueman JWH, Robinson A, Cockburn A. An unusual source of apparent mitochondrial heteroplasmy: duplicate mitochondrial control regions in *Thalassarche albatrosses*. *Molecular Ecology*. 2005; 14: 3605-13.
19. Simon C, Buckley TR, Frati F, Stewart JB, Beckenbach AT. Incorporating molecular evolution into phylogenetic analysis, and a new compilation of conserved polymerase chain reaction primers for animal mitochondrial DNA. *Annual Review of Ecology and Systematics*. 2006; 37: 545-79.
20. Staden R, Beal KF, Bonfield JK. The Staden package, 1998. *Methods in Molecular Biology*. 2000; 132: 115-30.
21. Lowe TM, Eddy SR. tRNAscan-SE: A program for improved detection of transfer RNA genes in genomic sequence. *Nucleic Acids Research*. 1997; 25: 955-64.
22. Cannone JJ, Subramanian S, Schnare MN, Collett JR, D'Souza LM, Du Y, Feng B, Lin N, Madabusi LV, Müller KM, Pande N, Shang Z, Yu N, Gutell RR. The Comparative RNA Web (CRW) site: an online database of comparative sequence and structure information for ribosomal, intron, and other RNAs. *BMC Bioinformatics*. 2002; 3: 2.
23. Clary DO, Wolstenholme DR. Drosophila mitochondrial DNA: Conserved sequences in the A + T-rich region and supporting evidence for a secondary structure model of the small ribosomal RNA. *Journal of Molecular Evolution*. 1987; 25: 116-25.
24. Tamura K, Peterson D, Peterson N, Stecher G, Nei M, Kumar S. MEGA5: Molecular evolutionary genetics analysis using maximum likelihood, evolutionary distance, and maximum parsimony methods. *Molecular Biology and Evolution*. 2011; 28: 2731-9.
25. Librado P, Rozas J. DnaSP v5: A software for comprehensive analysis of DNA polymorphism data. *Bioinformatics*. 2009; 25: 1451-2.
26. Benson G. Tandem repeats finder: A program to analyze DNA sequences. *Nucleic Acids Research*. 1999; 27: 573-80.
27. Zuker M. Mfold web server for nucleic acid folding and hybridization prediction. *Nucleic Acids Research*. 2003; 31: 3406-15.
28. Thompson JD, Gibson TJ, Plewniak F, Jeanmougin F, Higgins DG. The CLUSTAL X Windows interface: Flexible strategies for multiple sequence alignment aided by quality analysis tools. *Nucleic Acids Research*. 1997; 25: 4876-82.
29. Hall TA. BioEdit: A user-friendly biological sequence alignment editor and analysis program for Windows 95/98/NT. *Nucleic Acids Symposium Series*. 1999; 41: 95-8.
30. Posada D, Crandall KA. MODELTEST: testing the model of DNA substitution. *Bioinformatics*. 1998; 14: 817-8.
31. Nylander JAA. MrModeltest v2. Program distributed by the author. Uppsala University, Uppsala, Sweden, Evolutionary Biology Centre. 2004.
32. Ronquist F, Huelsenbeck JP. MrBayes 3: Bayesian phylogenetic inference under mixed models. *Bioinformatics*. 2003; 19: 1572-4.
33. Stamatakis A. RAxML-VI-HPC: maximum likelihood-based phylogenetic analyses with thousands of taxa and mixed models. *Bioinformatics*. 2006; 22: 2688-90.
34. Wang T, Yu P, Ma Y, Cheng H, Zhang J. The complete mitochondrial genome of *L. albella* (Mantodea: Iridopterygidae). *Mitochondrial DNA Part A*. 2016; 27: 465-6.
35. Buckley TR, Simon C, Flook PK, Misof B. Secondary structure and conserved motifs of the frequently sequenced domains IV and V of the insect mitochondrial large subunit rRNA gene. *Insect Mol Biol*. 2000; 9: 565-80.
36. Broughton RE, Dowling TE. Length variation in mitochondrial DNA of the minnow *Cyprinella spiloptera*. *Genetics*. 1994; 138: 179-90.
37. Buroker NE, Brown JR, Gilbert TA, O'Hara PJ, Beckenbach AT, Thomas WK, Smith MJ. Length heteroplasmy of sturgeon mitochondrial DNA: An illegitimate elongation model. *Genetics*. 1990; 124: 157-63.
38. Savolainen P, Arvestad L, Lundeberg J. mtDNA tandem repeats in domestic dogs and wolves: Mutation mechanism studied by analysis of the sequence of imperfect repeats. *Molecular Biology and Evolution*. 2000; 17: 474-88.
39. Cameron SL, Lambkin CL, Barker SC, Whiting MF. A mitochondrial genome phylogeny of Diptera: whole genome sequence data accurately resolve relationships over broad timescales with high precision. *Systematic Entomology*. 2007; 32: 40-59.
40. Pons J, Ribera I, Bertranpetit J, Balke M. Nucleotide substitution rates for the full set of mitochondrial protein-coding genes in Coleoptera. *Molecular Phylogenetics and Evolution*. 2010; 56: 796-807.
41. Zhang D, Yan LP, Zhang M, Chu HJ, Cao J, Li K, Hu DF, Pape T. Phylogenetic inference of calypteres, with the first mitogenomes for Gasterophilinae (Diptera: Oestridae) and paramacronychiinae (Diptera: Sarcophagidae). *International Journal of Biological Sciences*. 2016; 12: 489-504.
42. Ruokonen M, Kvist L. Structure and evolution of the avian mitochondrial control region. *Molecular Phylogenetics and Evolution*. 2002; 23: 422-32.
43. Yang J, Ye F, Huang Y. Mitochondrial genomes of four katydid (Orthoptera: Phaneropteridae): New gene rearrangements and their phylogenetic implications. *Gene*. 2016; 575: 702-11.
44. Boore JL. The duplication/random loss model for gene rearrangement exemplified by mitochondrial genomes of deuterostome animals. In: Sankoff D, Nadeau JH, eds. *Comparative genomics*. Dordrecht: Kluwer Academic Publishers; 2000: 133-147.
45. Tatarenkov A, Avise JC. Rapid concerted evolution in animal mitochondrial DNA. *Proceedings of the Royal Society B-Biological Sciences*. 2007; 274: 1795-8.
46. Moritz C, Brown WM. Tandem duplications in animal mitochondrial DNAs: variation in incidence and gene content among lizards. *Proceedings of the National Academy of Sciences, USA*. 1987; 84: 7183-7.
47. Svenson GJ, Whiting MF. Reconstructing the origins of praying mantises (Dictyoptera, Mantodea): the roles of Gondwanan vicariance and morphological convergence. *Cladistics*. 2009; 25: 468-514.
48. Legendre F, Nel A, Svenson GJ, Robillard T, Pellens R, Grandcolas P. Phylogeny of Dictyoptera: Dating the Origin of Cockroaches, Praying Mantises and Termites with Molecular Data and Controlled Fossil Evidence. *PLoS one*. 2015; 10: e0130127.